Effect of quasicrystalline phase on the deformation behavior of $Zr_{62}Al_{9.5}Ni_{9.5}Cu_{14}Nb_5$ bulk metallic glass

Y.F. Sun [a], T.L. Cheung [b], Y.R. Wang [a], C.H. Shek [b, *], W.H. Li [a], B.C. Wei [a]

[a] *National Microgravity Lab, Institute of Mechanics, Chinese Academy of Sciences, Beijing 100080, China*
[b] *Department of Physics and Materials Science, City University of Hong Kong, Hong Kong*

Abstract

Quasicrystalline phase with different volume fraction were formed by isothermally annealing the as-cast $Zr_{62}Al_{9.5}Ni_{9.5}Cu_{14}Nb_5$ bulk metallic glass at 723 K for different times. The effects of quasicrystals on the deformation behavior of the materials were studied by nanoindentation and compression test. It revealed that the alloys with homogeneous amorphous structure exhibit pronounced flow serrations during the nanoindentation loading, while no obvious flow serration is observed for the sample with quasicrystals more than 10 vol.%. However, further compression tests confirm that the no-serrated flows are formed due to different reasons. For annealed samples containing quasicrystals less than 35 vol.%, continuous plastic deformation occurs due to propagation of multiple shear bands. While the disappearance of serrated flow cannot be explained by the generation of multiple shear bands for samples containing quasicrystals more than 35 vol.%, which will fracture with a totally different fracture mode, namely, dimple fracture mode under loading instead of shear fracture mode.
© 2005 Published by Elsevier B.V.

Keywords: Quasicrystalline particles; Bulk metallic glass; Serrated flow; Nanoindentation

1. Introduction

The discovery of Bulk metallic glasses (BMGs) has sparked considerable interest due to their unique mechanical and physical properties, including high strength, relatively low Young's modulus and perfect elastic behavior. However, BMGs often show little global plasticity at room temperature, which is the major obstacle for being used as structural materials [1–5]. Extensive investigations have revealed that the limited room temperature plasticity is due to a catastrophic failure resulting from propagation of highly localized shear bands, which is considered to be the primary plastic deformation mechanism in metallic glass [6–8]. Recently, nanoindentation has been proposed as a useful way for the study of mechanical properties of BMGs at the length scale of shear bands, because under multiaxial compressive test, larger plastic deformation was allowed to accumulate around the indented regions in the materials. The materials often ex-

hibit serrated flow during nanoindentation, manifested as a stepped load–displacement (P–h) curve punctuated by discrete bursts of plasticity. The characters of serrations are strongly dependent on the indentation loading rate and are already found in Pd-, Zr- and La-based BMGs [9–11]. More recently, nanoindentation is used to study the plastic flow of BMGs containing crystalline particles. The second phase in the BMG can effectively resist the propagation of shear bands and the resistance can be reflected by the changes of serrated flow during nanoindentation [12,13].

It was known that the brittle crystalline particles contained in BMGs usually can not improve the plasticity [14,15], while the mechanical properties of the quasicrystalline contained metallic glass alloys have displayed very superior mechanical properties such as better ductility, along with high hardness value in comparison to its amorphous counterpart [16–19]. Therefore, investigation of the deformation behavior of the quasicrystals contained BMGs seems to be very important. In this paper, we report the formation of quasicrystalline particles after isothermally annealing the as-cast $Zr_{62}Al_{9.5}Ni_{9.5}Cu_{14}Nb_5$ bulk metallic glass. Nanoindentation

* Corresponding author. Tel.: +852 27887798; fax: +852 27887830.
E-mail address: apchshek@cityu.edu.hk (C.H. Shek).

and compression test were used to study the different plastic deformation behavior of the alloys.

2. Experimental procedure

Ingots of $Zr_{62}Al_{9.5}Ni_{9.5}Cu_{14}Nb_5$ were prepared by arc-melting a mixture of the pure elements Al, Ni, Cu and Zr–Nb intermediate binary alloy in a Ti-gettered argon atmosphere. Alloy rods of 3 mm in diameter and 70 mm in length were prepared from the pre-alloyed ingots by suction casting into a water-cooled copper mold. The structure of the as-cast alloy rods and annealed samples were characterized by X-ray diffraction (XRD) using Cu Kα radiation. Thermal analysis was performed at a heating rate of 20 K/min with a Perkin-Elmer DSC 7 differential scanning calorimeter under argon atmosphere. Microstructure of each sample was examined using a Jeol 5200 SEM and a Philips TECNAI 20 electron microscope operated at 200 kV. The compression test was carried out at a strain rate of $10^{-4}\,s^{-1}$ using an 8852 Instron-type testing machine. The specimens were carefully polished flat and parallel, with the aspect ratio of 2:1. The nanoindentation experiments were carried out with a constant loading rate of 10 mN/min on a nanoindenter supplied by CSM Instruments SA in Switzerland. The probe used was a Berkovich tip (CSM Instrument SA, Peseux, Switzerland). The nanoindenter has a maximum load of 300 mN, and the typical thermal drift rate is about 0.1 nm/s. To minimize surface variability and effects of thermal drift, large loads approaching the machine limit were used.

3. Experimental results

Fig. 1 shows the XRD patterns recorded for the cross-section of the as-cast $Zr_{62}Al_{9.5}Ni_{9.5}Cu_{14}Nb_5$ metallic glass
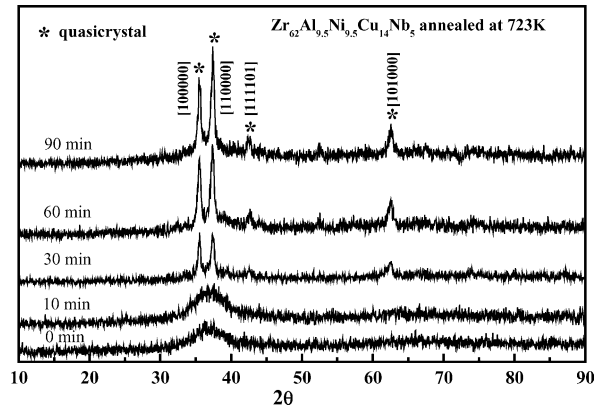

Fig. 1. X-ray diffraction pattern of the Zr-based alloys annealed for different time at 723 K.

and the samples annealed at 723 K for 10, 30, 60 and 90 min. It is clear that the samples annealed for 10 min are still amorphous, while the XRD pattern recorded for the samples annealed more than 10 min shows some obvious sharp diffraction peaks. Almost all the peaks can be identified as an icosahedral quasicrystalline phase. The strength of the quasicrystalline diffraction peaks becomes stronger with increasing annealed time and no other diffraction peaks were detected for the annealed samples.

SEM images of the as-cast sample and samples annealed for 30, 60 and 90 min are shown in Fig. 2. All the annealed samples exhibit a uniform distribution of quasicrystalline particles on the amorphous matrix. The volume fraction and size of the precipitated quasicrystalline particles increase with the increasing annealed time. For samples annealed for 30, 60 and 90 min, the volume fraction of quasicrystals are estimated to be about 10, 35, 65 vol.%, respectively. TEM images of the samples annealed for 90 min are shown in Fig. 3. The size of the quasicrystalline particles is about 200 nm, which is shown in Fig. 3(a). The corresponding selected
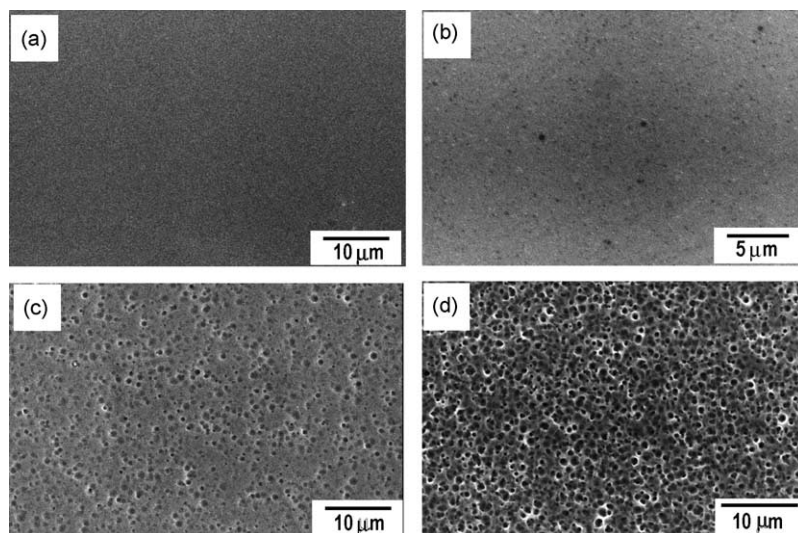

Fig. 2. SEM images showing the microstructure of the etched (a) as-cast sample and samples annealed at 723 K for (b) 30 min; (c) 60 min; (c) 90 min.
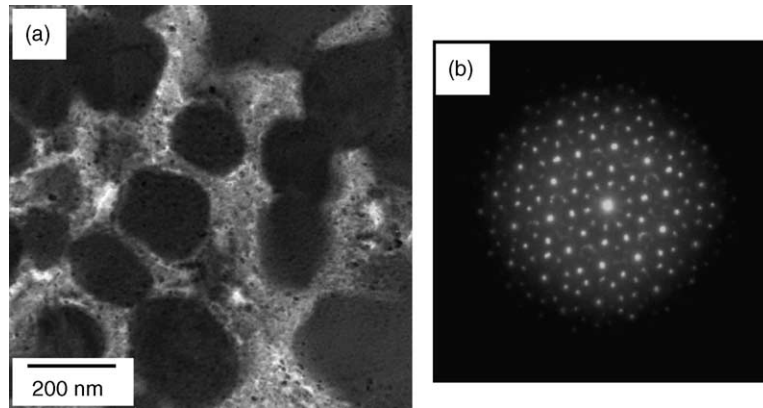
Fig. 3. TEM bright field images of the (a) annealed samples at 723 K for 90 min and (b) SAED pattern of the quasicrystalline phase.

area electron diffraction (SAED) pattern of the particles is shown in Fig. 3(b). The five-fold symmetry of the diffraction pattern corroborates the formation of quasicrystalline phase.

Plastic deformation behavior investigations by nanoindentation test reveal that a transition from serrated flow to no-serrated flow occurs among the samples. The nanoindentation $P–h$ curves for the samples are present in Fig. 4 as a typical example. Fig. 4(a) shows the complete $P–h$ plots including unloading curves, while Fig. 4(b) is a magnified portion of the curves of Fig. 4(a) for the sake of a better observation of the serrated flow changes on the curves. From Fig. 4(a), the shape of the curves for as-cast samples is quite similar to that of the annealed samples. However, the maximum indentation depth increases with increasing annealed time, indicating a gradual decrease of hardness. The hardness of the Zr-base alloys annealed for different times are listed in Table 1, which are obtained from the curves using Oliver–Pharr method. From the magnified section of the $P–h$ plots shown in Fig. 4(b), several displacement discontinuity or pop-in marks are found on the curves of the as-cast sample and 10 min annealed sample, illustrating a sadden penetration of the tip into the sample. The starting depth for the appearance of the distinct serrated flow

Table 1
Hardness of the Zr-based alloys annealed for different time at 723 K

Annealed time (min)	Hardness (GPa)
0	8.0
10	7.7
30	6.2
60	5.5
90	5.2

is about 700 and 800 nm, respectively. For samples annealed for more than 10 min, the serrated flow feature becomes very weak and gradually disappears with the increasing annealed time.

The transition of serrated flow for as-cast sample to no-serrated flow can also be confirmed by the surface deformation feature around the indent. Fig. 5 shows the SEM images of the typical surface deformation features obtained after nanoindentation of the as-cast sample and the samples annealed for 30 and 90 min. For as-cast sample, the representative indent in Fig. 5(a) is surrounded by characteristic circular patterns indicated by an arrow. As non-strain hardening materials, this plastically displaced material is
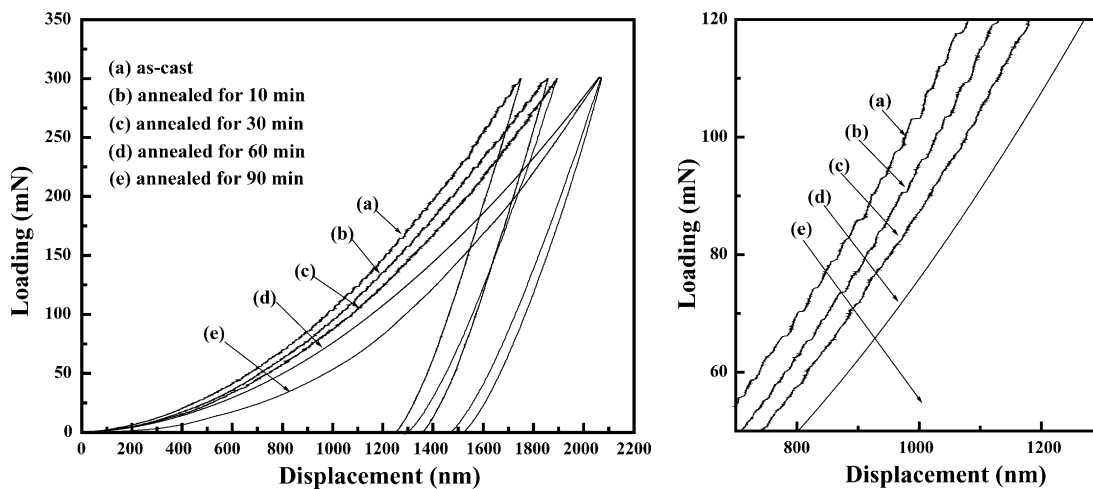

Fig. 4. Typical load–displacement ($P–h$) curved measurement of (a) as-cast sample and samples annealed for (b)10 min; (c) 30 min; (d) 60 min; (e) 90 min.
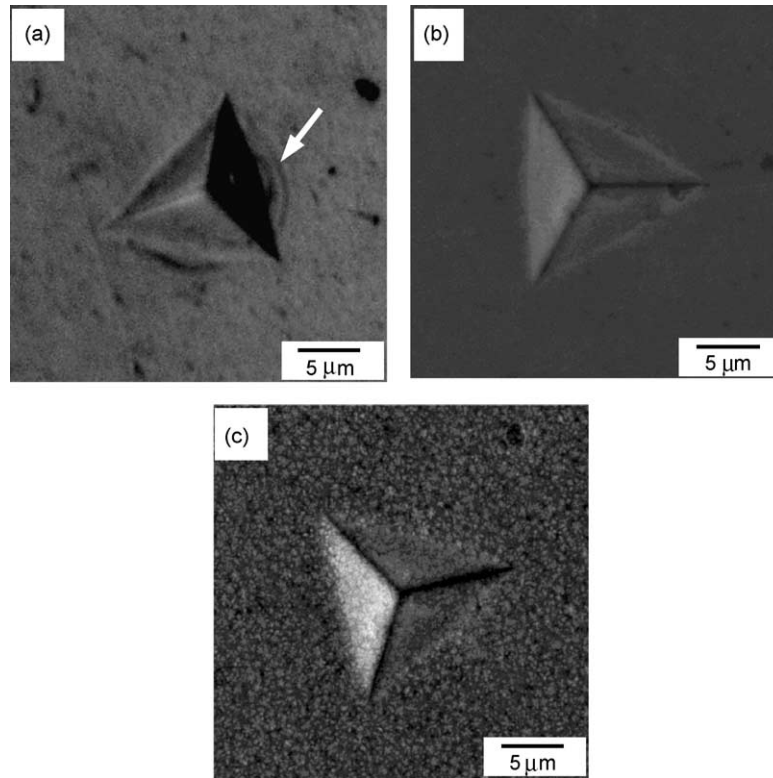
Fig. 5. SEM image showing the typical surface deformation features obtained from indents: (a) as-cast metallic glass; (b) sample annealed for 30 min; (c) sample annealed for 90 min.

expected to flow up to the faces of the indenter due to the incompressibility of plastic deformation. For annealed sample shown in Fig. 5(b) and (c), no obvious circular patterns can be observed around the indent.

Uniaxial compression tests of each sample were also conducted at room temperature, from which the stress–strain curves were obtained and shown in Fig. 6. From the stress–strain curves, the serrated flow can be observed for as-cast sample and samples annealed for 10 min. But for sam-

ples annealed for more than 10 min, no serrated flow can be observed. The variation of the serrations on the stress–strain curves agrees well with that of nanoindentation test. Fig. 7 exhibits the fracture surface of the as-cast sample, 30 and 90 min annealed sample after uniaxial compression test. The vein-like patterns in the fracture surface of the as-cast samples confirm a remarkable plastic flow before failure. However, for the 30 min annealed sample, no flow feature is found and multiple shear bands seem to be initiated. For 90 min annealed sample, dimples caused by falling off of quasicrystalline particles can be observed on the fracture plane, which indicates a dimple fracture mode occurs for this sample.

4. Discussions

In the present nanoindentation test, the *P–h* curves transforms from serrated for as-cast and 10 min annealed samples to smooth parabolic for samples annealed for more than 10 min, which seems as if a transition from discrete to continuous yield occurs among the samples. It is generally believed that the discrete pop-in events on the *P–h* curves correspond to the activation of individual shear bands. The disappearances of serrated flow on the *P–h* curves in monolithic BMG are usually found at high strain rate [20–22]. Because at slow strain rate, the applied strain can be accommodated by a single shear band resulting in a displacement step in the indentation curve, while at rapid loading rates, the applied strain rate
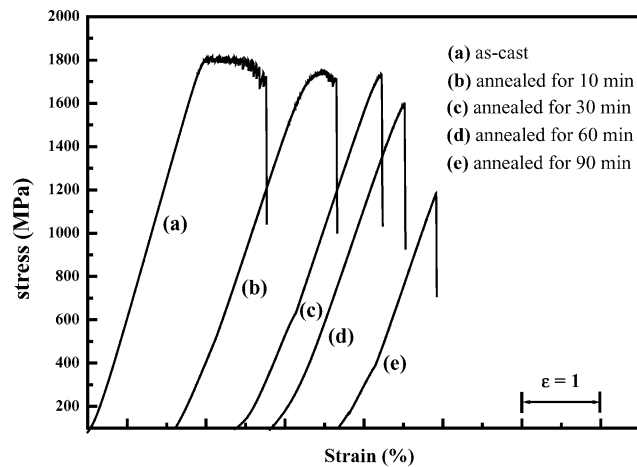

Fig. 6. Compression stress–strain curves of (a) as-cast sample and samples annealed for (b)10 min; (c) 30 min; (d) 60 min; (e)90 min at room temperature.
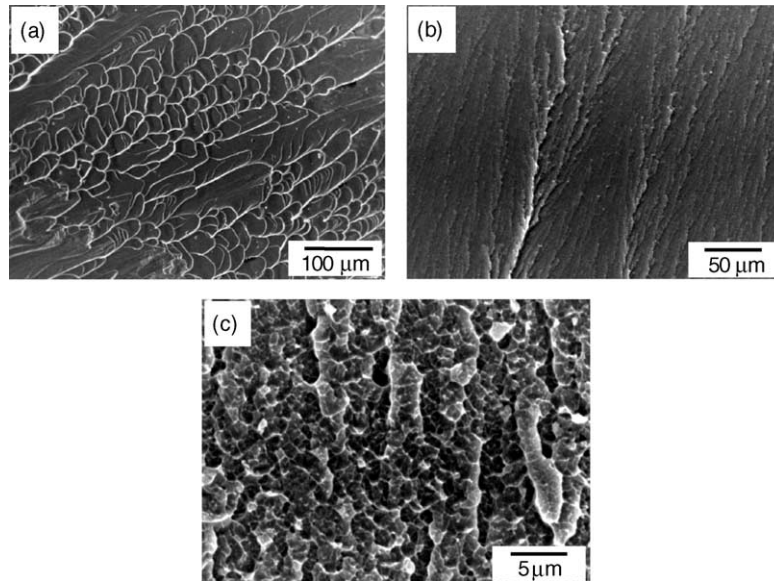
Fig. 7. SEM image of the fracture surface of the (a) as-cast sample; and (b) samples annealed for 30 min; (c) samples annealed for 90 min.

exceeds the rate of relaxation by a single band, more shear bands are required at every instant in order to continuously accommodate the applied stain, therefore, discrete steps in the indentation curve cannot be observed. Recently, it was found that the serrated flow could be remarkably affected by the microstructure, namely, the crystalline phase embedded in the amorphous matrix plays an important role in the serrated flow feature during the loading process of nanoindentation. It is pointed out that crystals larger than the shear band thickness can interfere with normal shear band nucleation and propagation [12,13]. The propagation of a single shear band is obstructed in a very limited scale, and many shear bands would be required at every instance in order to accommodate the applied strain. Since the thickness of shear band is nanometer-sized which is smaller than the size of quasicrystals in present paper, this size effect on the serrated flow can also be observed in present condition and can be confirmed by the morphology of the fractured plane. In Fig. 7(a), the vein-like feature for as-cast sample confirm obvious plastic flow before failure, while for sample annealed for 30 min shown in Fig. 7(b), no distinct flow feature is observed. However, in the present study, it is suggested that the volume fraction of the crystals simultaneously plays an important role in the shear bands operation. Although no serrated flow can be observed on the *P–h* curve, it cannot be explained that the generation and propagation of multiple shear bands occurs during the loading. If the crystals were too densely distributed in the amorphous matrix, the distance between the crystals becomes very small, resulting in great difficulties for the shear bands moving through the materials. On the other hand, since the shear bands are always accompanied by the generation and annihilation of the free volume in amorphous phase, the decrease of the volume fraction of amorphous matrix in the alloys with great amount of crystals would have more difficulties in giving rise to the formation of shear bands. As for 90 min annealed samples with quasicrystals about 65 vol.%, the bonding strength of the interface between the second phase and the amorphous will become more important. From the morphology of the fracture plane shown in Fig. 7(c), the materials fracture via a dimple fracture mechanism, instead of a shear fracture mode.

5. Conclusions

Quasicrystals with different volume fraction can be formed by isothermal annealing the as-cast $Zr_{62}Al_{9.5}Ni_{9.5}Cu_{14}Nb_5$ BMG for different time. Nanoindentation tests reveal that obvious flow serrations can be observed for as-cast alloys, while presence of quasicrystals remarkably retard the occurrence of the serrated flow. Further compressive test reveals that the disappearance of serrated flow might be caused by nucleation of multiple shear bands for annealed sample with small volume fraction of quasicrystals. However, different fracture mechanism, will apply for annealed alloys with high volume fraction of quasicrystals.

References

[1] E. Pekarskaya, C.P. Kim, W.L. Johnson, J. Mater. Res. 16 (2001) 2513.

[2] H.A. Bruck, T. Christman, A.J. Rosakis, W.J. Johnson, Scripta Metall. Mater. 30 (1994) 429.

[3] H. Kimura, T. Masumoto, Acta Metall. 31 (1983) 231.

[4] W.J. Wright, R.B. Schwarz, W.D. Nix, Mater. Sci. Eng. A 319–321 (2001) 229.

[5] W.J. Wright, R. Saha, W.D. Nix, Mater. Trans. JIM 42 (2001) 642.

[6] T.C. Hufnagel, C. Fan, R.T. Ott, J. Li, et al., Intermetallics 10 (2002) 1163.

[7] Z.F. Zhang, G. He, J. Eckert, L. Schultz, Phys. Rev. Lett. 91 (2003) 045505.

[8] K.M. Flores, R.H. Dauskart, Acta Mater. 49 (2001) 2527.

[9] C.A. Schuh, T.G. Nieh, Acta Mater. 51 (2003) 87.

[10] J.G. Wang, B.W. Choi, T.G. Nieh, C.T. Liu, J. Mater. Res. 15 (2000) 798.

[11] T.G. Nieh, C. Schuh, J. Wadsworth, Y. Li, Intermetallics 10 (2002) 1177.

[12] A.L. Greer, A. Castellero, S.V. Madge, I.T. Walker, J.R. Wilde, Mater. Sci. Eng. A 375–377 (2004) 1182–1185.

[13] B.C. Wei, T.H. Zhang, W.H. Li, Y.F. Sun, Y. Yu, Y.R. Wang, Intermetallics 12 (2004) 1239–1243.

[14] Z. Bian, G. He, G.L. Chen, Scripta Mater. 46 (2002) 407–412.

[15] A. Leonhard, L.Q. Xing, M. Heilmaier, NanoStruct. Mater. 10 (1998) 805–817.

[16] U. Koster, D. Zander, Triwikantoro. Mater. Sci. Forum. 343–346 (2000) 203–212.

[17] B.S. Murty, D.H. Ping, K. Hono, Appl. Phys. Lett. 76 (2000) 55–58.

[18] J. Saida, M. Matsushita, Appl. Phys. Lett. 75 (1999) 3497–3499.

[19] L.Q. Xing, J. Eckert, W. Loser, Appl. Phys. Lett. 73 (1998) 2110–2113.

[20] C.A. Schuh, T.G. Nieh, J. Mater. Res. 19 (2004) 46.

[21] N.Q. Chinh, J. Gubicza, Z. Kovacs, J. Lendvai, J. Mater. Res. 19 (2004) 31.

[22] C.A. Schuh, A.S. Argon, T.G. Nieh, J. Wadsworth, Philosophical Mag. 83 (2003) 2585.